A Raman spectral study of forsterite-monticellite solid solutions

KAKKALA MOHANAN, SHIV K. SHARMA

Hawaii Institute of Geophysics, School of Ocean and Earth Science and Technology, University of Hawaii,
2525 Correa Road, Honolulu, Hawaii 96822, U.S.A.

FINLEY C. BISHOP

Department of Geological Sciences, Northwestern University, Evanston, Illinois 60208, U.S.A.

ABSTRACT

Raman spectra of olivines along the forsterite-monticellite (Fo-Mo) join have been measured in the region of 100–1200 cm^{-1} with a multichannel micro-Raman spectrometer. In the spectrum of Fo, strong Si-O$^-$ symmetric stretching bands appear at 824 and at 855 cm^{-1}, and a medium-intensity antisymmetric Si-O$^-$ stretching band appears at 964 cm^{-1}. These bands show a systematic frequency decrease with increasing Mo composition. These systematic variations of the high-frequency Si-O$^-$ bands are attributed to decreased distortion of SiO$_4$ tetrahedra. The mixing characteristics of the ν_1 and ν_3 modes in orthosilicates were found to depend strongly on the ratio of intertetrahedral $\langle$O-O$\rangle$ to $\langle$Si-O$\rangle$ bond lengths. In the low-frequency region of the spectra, Fo-rich compositions show progressive broadening of the bands with the addition of up to 16 wt% monticellite. But there is no appreciable broadening of the bands in the spectra of Mo-rich samples containing up to 18% Fo. The broadening of the low-frequency bands with increasing Mo component in the solid solution may be attributed to increasing positional disorder caused by the substitution of large Ca ions on the M1 octahedral sites.

INTRODUCTION

Olivines are considered to be one of the important constituents of the Earth's upper mantle and of meteorites. Among this large, well-studied class of orthosilicates, forsterite is one of the most common. In the ternary system containing forsterite (Mg$_2$SiO$_4$), fayalite (Fe$_2$SiO$_4$), and calcium olivine (Ca$_2$SiO$_4$), forsterite forms a complete solid solution with fayalite but not with the calcium olivine. In fact, under ambient conditions, it does not form a complete solid solution series with the intermediate isostructural mineral, monticellite, CaMgSiO$_4$ (Biggar and O'Hara, 1969; Brown, 1980). Knowledge of the structural behavior, such as cation disorder caused by varying cation content, is important to our understanding of geochemical and petrological systems. Adams and Bishop (1985) have studied the Fo-Mo solid solution series samples with X-ray diffraction techniques and detected only a small degree of Ca-Mg disorder.

Vibrational frequencies are very sensitive to interatomic forces. Raman and infrared (IR) spectroscopy could thus reveal small changes in bond lengths and bond angles of crystals responding to changes in composition, temperature, and pressure. These techniques have been used for both quantitative and qualitative analyses of minerals (Farmer, 1974), and the vibrational spectra of olivine have been extensively studied. Tarte (1963) and Burns and Huggins (1972) investigated IR spectra of several olivines. Huggins (1973) used vibrational spectra as

a tool to study cation ordering in olivine. Servoin and Piriou (1973) investigated both IR and Raman spectra of the solid solutions of (Mg$_{1-x}$Ni$_x$)$_2$SiO$_4$ and Mg$_2$(Si$_{1-x}$Ge$_x$)O$_4$ and identified the ν_1, ν_3, and ν_4 modes. Piriou and McMillan (1983) studied the high-frequency vibrational spectra of several orthosilicates and investigated the nature of the ν_1 and ν_3 mixing characteristics. Iishi (1978) modeled interatomic forces in Fo single crystals using vibrational data.

Raman spectra of a number of end-member olivines have been summarized and reported (Piriou and McMillan, 1983). Chopelas (1991) measured polarized single-crystal spectra of forsterite, fayalite, and monticellite and refined the existing observed vibrational data, but little work has been done on the effect of cation disorder on Raman spectra. Isotopic exchange experiments on orthosilicates (Paques-Ledent and Tarte, 1973) showed inconsistency in the assignments of the high-frequency vibrational modes. These workers concluded that there is strong coupling between the ν_1 and ν_3 modes in the vibrational spectra of orthosilicates. Recent theoretical work by Lam et al. (1990) showed that the ν_1 and ν_3 mixing in orthosilicates could be explained by considering both the corresponding $\langle$Si-O$\rangle$ bond length and the ratio of the average intratetrahedral O-O distance to the corresponding $\langle$Si-O$\rangle$ bond distance. In this work the Fo-Mo samples used in the previous X-ray studies have been probed with Raman spectroscopy to determine structural implications of systematic variations of composition, mixing

TABLE 1. Observed Raman frequencies for the Fo-Mo solid-solution series

Mode	Fo_{100}	Fo_{93}	Fo_{88}	Fo_{84}	Fo_{18}	Fo_{14}	Fo_6	Mo*
A_g	964.0(m)	963.1(m)	961.7(m)	961.7(m)	949.7(m)	949.7(m)	948.4(m)	949.0
B_{3g}	919.0(w)	917.7(w)	916.3(w)	915.0(w)	901.6(m)	900.2(m)	898.9(m)	900.0
A_g	855.0(vs)	854.5(vs)	853.2(vs)	851.8(vs)	847.8(vs)	847.8(vs)	850.5(vs)	851.0
A_g	824.0(s)	822.0(s)	819.5(s)	818.1(s)	816.8(s)	816.8(s)	816.8(s)	818.0
A_g	608.0(w)	606.0(w)	604.0(w)	603.9(w)	595.0(w)	592.0(w)	589.0(w)	589.0
$B_{1g} + B_{2g} + B_{3g}$	589.0(w)	586.8(w)	586.1(w)	586.3(w)	575.2(w)	580.0(w)	580.0(w)	560.0
A_g	544.0(w)	544.0(w)	543.7(w)	544.3(w)	575.3(w)	578.0(w)	578.0(w)	534.0
$B_{1g} + B_{2g} + B_{3g}$	433.5(w)	432.1(w)	429.4(w)	427.9(w)	415.0(s)	413.0(s)	409.5(s)	407.0
B_{3g}	374.0(w)	369.1(w)	368.0(w)	367.8(w)	—	—	—	266.0
A_g	337.0(w)	333.0(w)	327.4(w)	327.3(w)	336.3(w)	337.0(w)	337.0(w)	275.0
A_g	329.0(w)	—	—	—	—	—	—	307.0
B_{3g}	314.0(vw)	—	—	311.6(w)	313.6(w)	313.6(w)	307.5(w)	251.0
A_g	303.0(w)	298.6(w)	297.2(w)	295.9(w)	261.6(m)	260.9(m)	256.8(m)	258.0
A_g	225.0(w)	223.0(w)	216.5(w)	216.5(w)	—	—	214.4(w)	172.0

Note: vs = very strong; s = strong; m = medium; w = weak; vw = very weak.
* Data from Chopelas (1991).

characteristics of the high frequency modes, and order-disorder phenomena. We have used Raman spectroscopy for analysis of the samples along the Fo-Mo join because the Raman spectra of crystalline materials usually give rise to well-defined narrow bands and, therefore, both the frequencies and band widths can be used to examine the effect of composition and degree of disorder.

EXPERIMENTAL METHODS

The samples were synthesized under high pressure in a piston-cylinder solid-media apparatus and characterized with X-ray diffraction analysis (Adams and Bishop, 1985). Raman spectra of six polycrystalline forsterite-monticellite solid solution samples, ranging from 100 to 6 mol% Fo, were measured with a multichannel micro-Raman spectrometer. The spectra were obtained at a scattering geometry of 135° (Sharma and Urmos, 1987; Sharma, 1989). The 135° laser-excitation geometry has proved to give a better signal to noise ratio for a given sample than the 180° excitation geometry using the same spectroscopic parameters (Cooney and Sharma, 1990). The samples were excited using a 488-nm laser line from a Spectra Physics model 165 Ar⁺ ion laser. Laser power at the sample was 20 mW. A spectral resolution of 4 cm⁻¹ was used. In order to achieve a good signal to noise ratio in the spectra, 1000 scans, each of 4-s exposure, were added. The frequencies of Raman bands are accurate to ±0.6 cm⁻¹.

SYMMETRY ANALYSIS

Olivine has an orthorhombic structure and belongs to space group *Pbnm* (point group D_{2h}; $Z = 4$). Factor group analysis predicts the following 84 normal modes for this structural group (e.g., Lam et al., 1990):

$$\Gamma_{tot} = 11A_g \ (R) + 11B_{1g} \ (R) + 7B_{2g} \ (R) + 7B_{3g} \ (R)$$
$$+ 10A_u \ (ia) + 10B_{1u} \ (ir) + 14B_{2u} \ (ir)$$
$$+ 14B_{3u} \ (ir)$$

where R indicates the Raman active mode, ir, the infrared active mode, and ia, the inactive mode. The frequen-cies of the observed Raman spectra of polycrystalline powdered samples of Fo-Mo solid solution series are given in Table 1. Observation of fewer than anticipated Raman bands of the powdered samples is attributed to the weak intensities of some bands, as well as to accidental degeneracies of the bands, including the tendency of weak bands to merge with adjacent bands.

RESULTS AND DISCUSSION

High-frequency spectra

The Raman spectra of Fo-Mo solid solution series in the high-frequency region, 700–1000 cm⁻¹, are shown in Figure 1a. The high-frequency bands in the spectra of olivines are attributed to the ν_1 and ν_3 stretching vibrations of SiO_4 tetrahedra. A very weak shoulder at 880 cm⁻¹ is visible in the spectra of the Fo-rich end, but it merges with the 855 cm⁻¹ band in the Mo-rich end. Another weak feature, seen at 749 cm⁻¹ in the Mo-rich end, is not present in the Fo-rich olivine. The striking feature of these bands is the systematic variation of the frequency with composition. For example, starting from Fo-rich olivine to Mo-rich olivine, the bands at 824, 855, and 964 cm⁻¹ shift toward lower frequencies by approximately 5.4, 8.1, and 16 wavenumbers, respectively. This systematic frequency shift is largely due to the increase in the inter-tetrahedral O-O bond lengths as a result of the substitution of larger cations in the M2 sites (see below). The X-ray data (Adams and Bishop, 1985) indicate an increase up to 19% in the unit-cell volume from the Fo-rich to Mo-rich olivine. Replacement of Mg cations with Ca at the M2 site causes increases in the unit-cell parameters; in turn, the intertetrahedral O-O distance increases and SiO_4 tetrahedra become more relaxed (Lam et al., 1990). At the forsterite end, Raman frequency decreases linearly with composition, whereas in the monticellite end the Raman frequency increases, resulting in a reverse trend (Fig. 2). The intermediate solid solutions along the Fo-Mo join are not stable; as a result, we were not able to examine their Raman spectra. The coefficients of a linear fit to our data are given below. For convenience, the
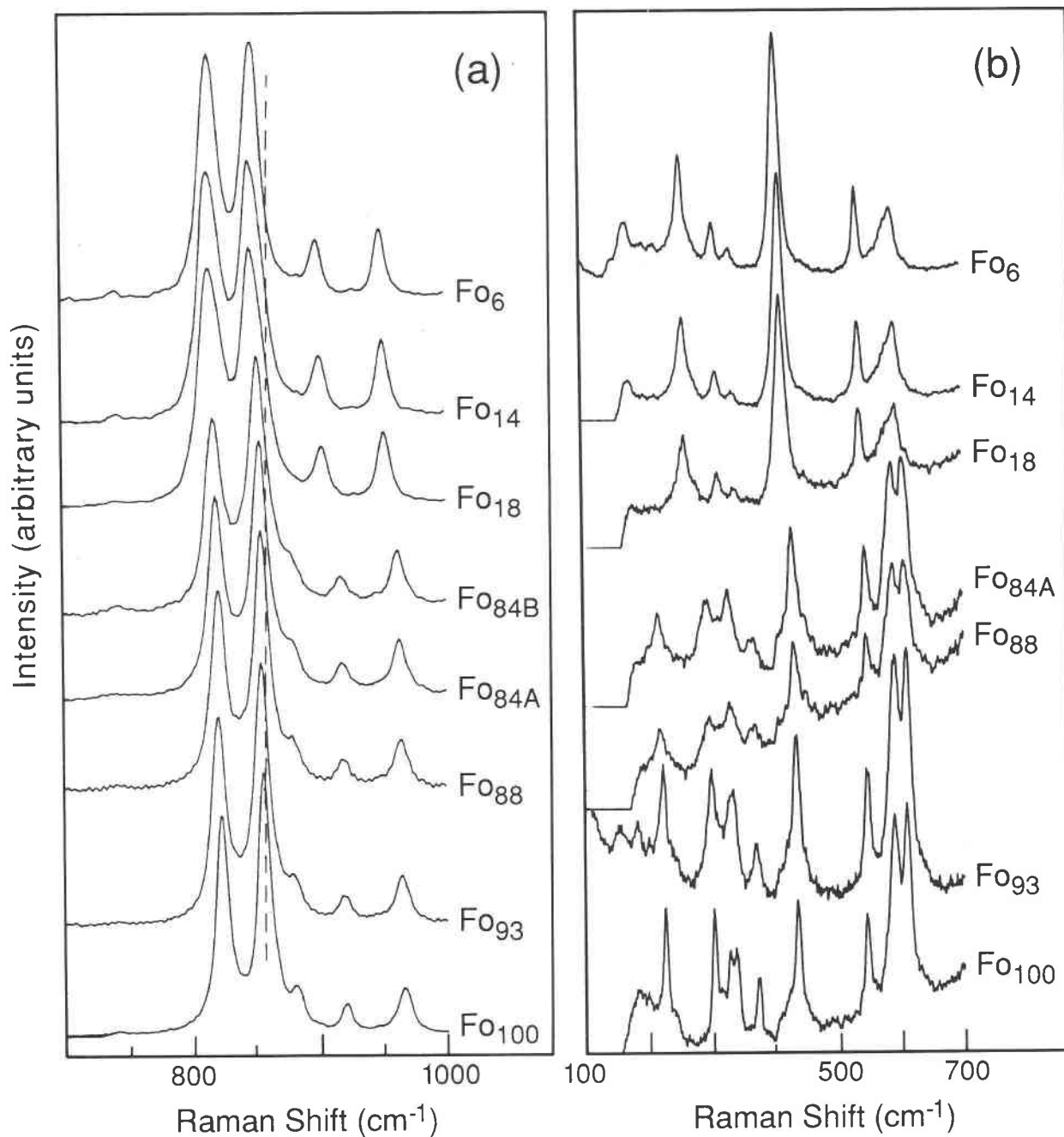
Fig. 1. (a) In the high frequency region (700–1000 cm^{-1}), the major bands at 964, 855, and 824 cm^{-1} are assigned to the stretching modes of the Si-O(1), Si-O(3), and Si-O(2) bonds, respectively. (b) The details of the Raman spectra of Fo-Mo solid solutions in the low frequency region (100–700 cm^{-1}).

equations are normalized to their respective end-member volume. Those with a forsterite-rich composition are

$$\nu_1 = 963.99 - 0.343V \qquad R = 0.963$$
$$\nu_2 = 855.34 - 0.432V \qquad R = 0.954$$
$$\nu_3 = 824.17 - 0.822V \qquad R = 0.995.$$

Those with a monticellite-rich composition are

$$\nu_1 = 948.50 + 0.205V \qquad R = 0.939$$
$$\nu_3 = 850.29 + 0.426V \qquad R = 0.939$$
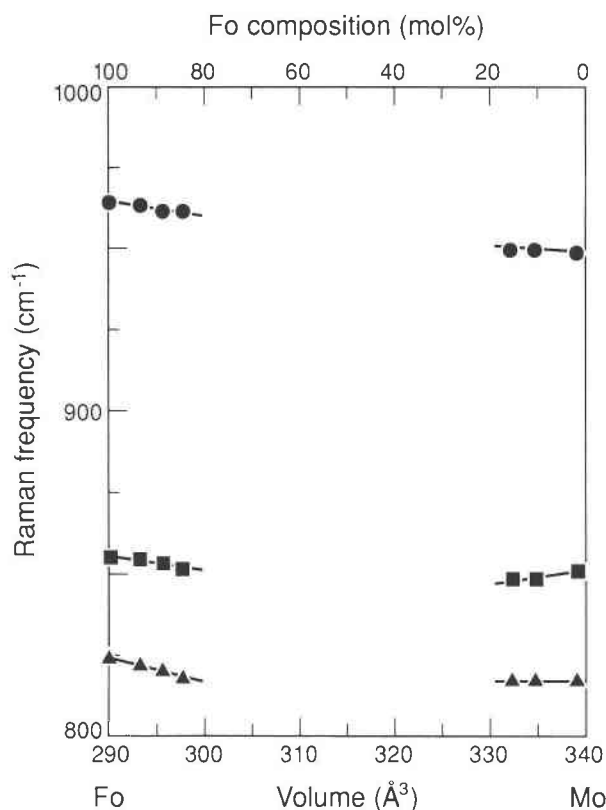$$\nu_2 = 816.80 \qquad \text{constant with respect to volume.}$$

Fig. 2. High frequency bands vs. unit-cell volume. Sample composition is given at the top of the abscissa. Legends: circle = 964 cm^{-1}; square = 855 cm^{-1}; and triangle = 824 cm^{-1}.

For all the equations, V is the unit-cell volume in the range 290–340 Å^3. The nonlinear behavior of the high-frequency bands is due to the complex nature of the vibrations of the SiO$_4$ tetrahedra that exist in the family of olivines (Piriou and McMillan, 1983). The linear correlation coefficients (R) for Mo are not very high, indicating that frequency variation of coupled ν_1-ν_3 modes with volume are not linear.

Let us consider the behavior and characteristics of the high-frequency bands in the Fo-Mo solid solution series. The bands of interest for Fo in this study are the two intense A$_g$ modes at 855 and 824 cm^{-1} and the medium band at 964 cm^{-1}, originating from the stretching modes of SiO$_4$ tetrahedra. The lattice dynamics of Fo have attracted the attention of a number of workers (e.g., Price and Parker, 1984; Price et al., 1987; Rao et al., 1987; Lam et al., 1990). It is proposed that the band at 964 cm^{-1} contains large contributions from Si-O(1) bond stretch (Lam et al., 1990). The stretching bands at 855 and 824 cm^{-1} originate largely from Si-O(3) and Si-O(2) bonds, respectively. Their frequencies and half widths vary systematically with the cation content.

In general, the observed frequency of a bond-stretching vibration mode is inversely proportional to the corresponding bond length. In solids, however, such a simple relationship may not be strictly valid because of near-neighbor interactions and crystal field effects. Table 2 lists the Si-O bond lengths, the ratio of average intertetrahedral O-O distances to the Si-O bond distances, and the observed Raman frequencies in forsterite, monticellite, and calcium olivine. It is evident that within each of these minerals, a given vibrational band varies strongly as a function of corresponding inverse bond length. For example, in forsterite, this dependence is clear: for bond lengths Si-O(1) (1.620 Å), Si-O(3) (1.636 Å), and Si-O(2) (1.656 Å), the corresponding frequencies are 964, 855, and 824 cm^{-1}, respectively. But among other olivine crystal structures, a simple consideration of the bond lengths of the Si-O bonds alone does not explain the observed frequencies. To resolve this dilemma, Piriou and McMillan (1983) investigated the high-frequency vibrational spectra of several orthosilicates. They studied the vibrational coupling of the ν_1 and ν_3 modes by considering simple harmonic oscillators. Their simple theoretical model showed that the high-frequency vibrational modes vary with some physical parameter, X. They found that the strong band A$_g$ at 856 cm^{-1} in forsterite has more ν_1 character, whereas in the monticellite spectrum the band at 814 cm^{-1} has more ν_1 character. Among orthosilicates, monticellite lies closest to the crossover between ν_1 and ν_3 modes. It has therefore been suggested that in monticellite the mixing characteristics of ν_1 and ν_3 modes are more or less equal, and forsterite and calcium olivine are at the extremes (Piriou and McMillan, 1983).

The simple theoretical model of Piriou and McMillan (1983) explained the behavior of the ν_1 and ν_3 modes of olivines, but the relationship of the physical parameter X to the crystal structure was not clear. Lam et al. (1990) theoretically simulated the forsterite structure using a pair-

TABLE 2. Variation of the high-frequency Si-O stretching modes with their respective bond lengths and the ratio of intertetrahedra ⟨O-O⟩ to Si-O interactions

	Fo			Mo			Ca		
Bond	Bond length (Å)	⟨O-O⟩ Si-O	Frequency (cm^{-1})	Bond length (Å)	⟨O-O⟩ Si-O	Frequency (cm^{-1})	Bond length (Å)	⟨O-O⟩ Si-O	Frequency* (cm^{-1})
Si-O(1)	1.620	1.840	964.0	1.615	1.957	949.0	1.637	2.0504	925.0
Si-O(3)	1.636	1.822	856.0	1.640	1.927	851.0	1.642	2.0442	839.4
Si-O(2)	1.656	1.800	824.0	1.656	1.908	817.0	1.665	2.0159	813.6

Note: The mixing of ν_1 and ν_3 modes in olivines is a combined effect of the two factors tabulated here.
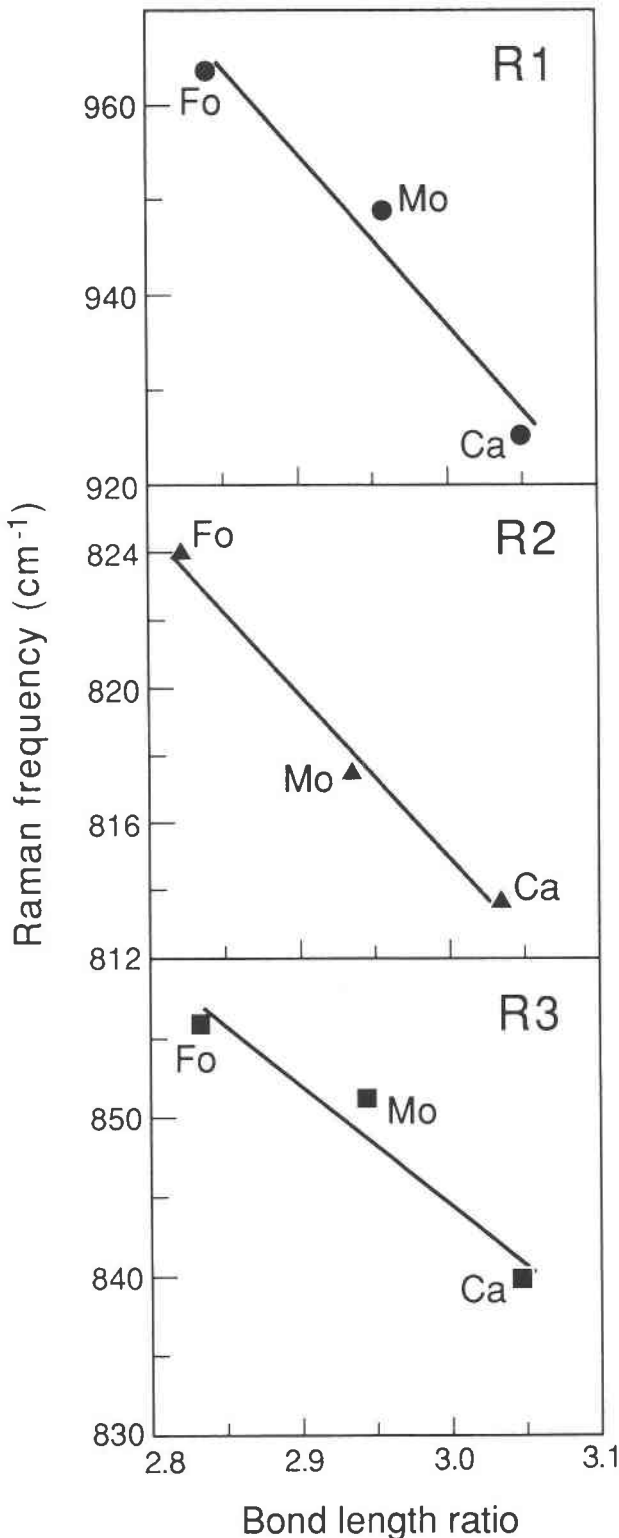* Data from Piriou and McMillan (1983).

Fig. 3. The dependence of high-frequency bands in olivines on the sum of the ratio of Si-O bond lengths to the Si-O(1) bond length and the ratio of intertetrahedral lengths to the Si-O bond lengths. Bond length ratio: R1 = [Si-O(1)]/[Si-O(1)] + ⟨O-O⟩/[Si-O(1)]; R2 = [Si-O(2)]/[Si-O(1)] + ⟨O-O⟩/[Si-O(2)]; R3 = [Si-O(3)]/[Si-O(1)] + ⟨O-O⟩/[Si-O(3)].

potential model by taking into account the ionic and covalent interactions, as well as the core-core repulsion forces. Their model shows that the high-frequency ν_1 and ν_3 modes of olivine are not only affected by the variations of the Si-O bond but also by the variation of intertetrahedral O-O interactions. Lam et al. (1990) showed that the intertetrahedral O-O distance varies by 10% with the substitution of larger cations. They proposed that the intensity of ν_1 and ν_3 mixing is attributed to the net effect of the intertetrahedral ⟨O-O⟩ force constant and the Si-O force constant.

We have calculated the ratios of intertetrahedral ⟨O-O⟩ to ⟨Si-O⟩ distances for forsterite, monticellite, and calcium olivine and tabulated them, along with the Si-O bond lengths and their corresponding frequencies (see Table 2). It is noted that for a given composition, both across and down the table, the lower the value of this ratio, the higher the Raman frequency. When a larger cation is substituted into the forsterite structure, Si-O bond length increases, and the relative degree of covalency of the bond decreases. Moreover, the intra- and intertetrahedral ⟨O-O⟩ distances increase. When the Raman frequencies 964, 855, and 824 cm^{-1} of Fo and the corresponding band frequencies of Mo and calcium olivine are plotted with the sum of the ratio of the corresponding Si-O bond length to the Si-O(1) bond length and the ratio of intertetrahedral ⟨O-O⟩ to ⟨Si-O$_n$⟩ distances (where n = 1, 2, 3) in the respective mineral (Fig. 3), a good linear trend is shown, with forsterite having the highest value of these modes and calcium olivine having the lowest. Our present Raman data on Fo-Mo solid solutions are therefore in agreement with the predictions of Lam et al. (1990).

Low-frequency spectra

Raman spectra of the Fo-Mo series in the low-frequency region, 100–700 cm^{-1} (Fig. 1b) show band broadening, a systematic decrease in frequency, and the merging of adjacent bands. Frequencies of these bands shift toward lower wavenumbers as the composition of the solid solution varies across the Fo-Mo join. The bands are fairly sharp in the Mo-rich samples but broad in the Fo-rich samples.

In vibrational spectroscopy, the half width of a band is used to study positional disorder in crystal structures. Two strong bands at 433.5 and 544 cm^{-1} are assigned, respectively, as a B-type mode and an A_g mode originating from ν_4 vibrations. We have selected these bands because they have relatively strong intensities and have flat base lines for half-width calculations. Even though the band at 433.5 cm^{-1} could be a combination of the B_{1g} + B_{2g} + B_{3g} modes, in the spectra of polycrystalline samples the intensities of the B_{2g} and B_{3g} modes are usually much weaker than that of the B_{1g} mode, and therefore the selection of the 433.5-cm^{-1} band for half-width calculation is justifiable. On the addition of Ca, these bands show broadening in the Fo-rich samples and narrowing in the Mo-rich samples. For example, at the forsterite end, the 433.5-cm^{-1} band has a half width of 11.5 cm^{-1}, and it

increases by seven wavenumbers with the addition of 16 mol% Ca (Fig. 4). On the other hand, in the Mo-rich end, its half width decreases by one wavenumber with the addition of 8 mol% Ca. The same behavior is observed with the 544-cm^{-1} band. This unusual behavior can be explained on the basis of order-disorder phenomena in the crystal. Positional disorder in binary olivine is caused by the occupancy of larger cations, such as Ca (ionic radii 1.0 Å), in the smaller M1 site. In forsterite, the two structural sites M1 and M2 are of the same size. In monticellite, the M2 site is larger than the M1 site. By preference, the larger cation (Ca) fills the M2 site and the smaller cation (Mg) the M1 site. For this reason, monticellite is a highly ordered mineral. The addition of Ca to forsterite affects its crystal structure in two ways: the occupancy of either site by Ca distorts the crystal structure and hence the SiO$_4$ tetrahedra and the presence of Ca in both M1 and M2 sites introduces positional disorder into the crystal structure. On the other hand, in monticellite, the M2 site is already big enough to accommodate the Mg ion without affecting the crystal structure, but it does introduce disorder. For these reasons, the addition of Ca into the forsterite-rich composition causes considerable increase in the half width of the Raman bands, whereas in the monticellite end, addition of Mg causes only a slight increase in the half width. Adams and Bishop (1985) determined the presence of a maximum of 11% Ca in the M1 site in the Fo-rich samples and 2% Ca in the Mo-rich samples. A comparison of the observed change (Fig. 4) in the slope of the bands of SiO$_4$ near the Fo end to those of minerals near the Mo end further indicates that Fo-rich olivines exhibit higher (Ca,Mg) disorder. Disorder in general tends to decrease the frequencies of the Raman bands.

In silicate solid solutions, we expected to observe a negative excess-volume effect (Newton and Wood, 1980). The data of Adams and Bishop (1985), however, show a nearly linear relationship between the unit-cell volume and composition across the given end-members. The absence of such excess-volume effects in these samples implies that the substitution of the larger Ca cation at the M1 site in the Fo end causes the volume to increase linearly. It is, however, evident from Figure 2 that the frequencies of the high-frequency bands of SiO$_4$ are not linearly dependent on unit-cell volume along the Fo-Mo join.

CONCLUSIONS

The Raman spectra of crystalline samples along the Fo-Mo join show well-defined bands. Analysis of the bands in the high-frequency (700–1000 cm^{-1}) region provide information about the mixing of ν_1 and ν_3 internal modes of SiO$_4$ tetrahedra. The 964 cm^{-1} band of Fo, which has a pure ν_3 character, decreases linearly from Fo to Mo, indicating decreased distortion of the SiO$_4$ tetrahedra. The 824 and 855 cm^{-1} bands of Fo do not show linear relationships with composition along the join, most likely because of the mixed ν_1 and ν_3 character of these bands.
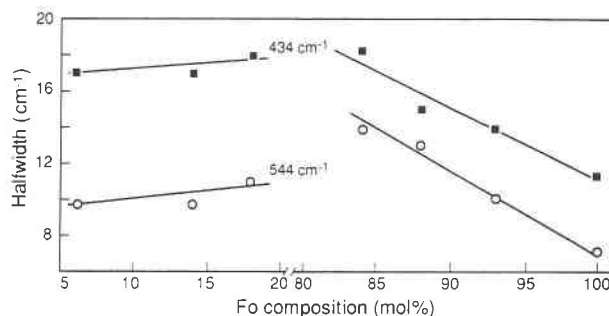

Fig. 4. Variation of half width for two major low-frequency bands, 433.5 and 544 cm^{-1}. In the Fo-rich compositions the steep slope is due to the substitution of larger cations in the M1 site (see text).

The mixing between the ν_1 and ν_3 modes is correlated with the following structural parameters of olivine: the respective bond length and the ratio of the average bond length of the O-O bond to the corresponding Si-O bond length.

In the low-frequency region, the A$_{1g}$ and B$_{1g}$ modes show significant broadening on substituting Ca^{2+} for Mg^{2+}, indicating that some of the Ca^{2+} ions occupy the M1 site. The substitution of Mg in the Mo crystal, however, causes only small variation in the half width of the low-frequency modes, indicating a smaller degree of Ca-Mg disorder near the Mo end.

In summary, the present study has shown that Raman spectroscopy not only is a sensitive tool for examining distortion of SiO$_4$ tetrahedra but also provides information about cation disorder in crystals.

REFERENCES CITED

Adams, G.E., and Bishop, F.C. (1985) An experimental investigation of thermodynamic mixing properties and unit-cell parameters of forsterite-monticellite solid solutions. American Mineralogist, 70, 714–722.

Biggar, G.M., and O'Hara, M.J. (1969) Monticellite and forsterite crystalline solutions. Journal of the American Ceramic Society, 52, 249–252.

Brown, G.E. (1980) Olivines and silicate spinels. In Mineralogical Society of America Reviews in Mineralogy, 5, 275–381.

Burns, R.G., and Huggins, F.E. (1972) Cation determinative curves for Mg-Fe-Mn olivines from vibrational spectra. American Mineralogist, 57, 967–985.

Chopelas, A. (1991) Single crystal Raman spectra of forsterite, fayalite, and monticellite. American Mineralogist, 76, 1101–1109.

Cooney, F.T., and Sharma, S.K. (1990) Structure of glasses in the systems Mg$_2$SiO$_4$-Fe$_2$SiO$_4$, Mn$_2$SiO$_4$-Fe$_2$SiO$_4$, Mg$_2$SiO$_4$-CaMgSiO$_4$, Mn$_2$SiO$_4$-CaMnSiO$_4$. Journal of Non-Crystalline Solids, 122, 10–32.

Farmer, V.C., Ed. (1974) The infrared spectra of minerals, 539 p. Mineralogical Society, London.

Huggins, F.E. (1973) Cation order in olivines: Evidence from vibrational spectra. Chemical Geology, 11, 99–109.

Iishi, K. (1978) Lattice dynamics of forsterite. American Mineralogist, 63, 1198–1208.

Lam, P.K., Yu, R., Lee, M.W., and Sharma, S.K. (1990) Relationship between crystal structure and vibrational mode in Mg_2SiO_4. American Mineralogist, 75, 109–119.

Newton, R.C., and Wood, B.J. (1980) Volume behavior of silicate solid solutions. American Mineralogist, 65, 733–745.

Paques-Ledent, M.Th., and Tarte, P. (1973) Vibrational studies of olivine-type compounds. I. The i.r. and Raman spectra of the isotopic species of Mg_2SiO_4. Spectrochimica Acta, 29A, 1007–1016.

Piriou, B., and McMillan, P. (1983) The high frequency vibrational spectra of vitreous and crystalline orthosilicates. American Mineralogist, 68, 426–443.

Price, D.G., and Parker, S.C. (1984) Computer simulations of the structural and physical properties of the olivine and spinel polymorphs of Mg_2SiO_4. Physics and Chemistry of Minerals, 10, 209–216.

Price, G.D., Parker, S.C., and Maurice, L. (1987) The lattice dynamics of forsterite. Mineralogical Magazine, 51, 157–170.

Rao, K.R., Chaplot, S.L., Choudhury, N., Ghose, S., and Price, D.L. (1987) Phonon density of states and specific heat of forsterite, Mg_2SiO_4. Science, 236, 64–65.

Servoin, J.L., and Piriou, B. (1973) Infrared reflectivity and Raman scattering of Mg_2SiO_4 single crystal. Physica Status Solidi, 55 B, 677–686.

Sharma, S.K. (1989) Applications of advanced Raman spectroscopic techniques in earth sciences. In H.D. Bist, J.R. Durig, and J.F. Sullivan, Eds., Raman spectroscopy: Sixty years on—Vibrational spectra and structure, p. 513–568. Elsevier, New York.

Sharma, S.K., and Urmos, J.P. (1987) Micro-Raman spectroscopic studies of materials at ambient and high pressures with cw and pulse lasers. In Roy H. Geiss, Ed., Microbeam analysis, p. 133–136. San Francisco Press, San Francisco.

Tarte, P. (1963) Etude infra-rouge des orthosilicates et des orthogermanates. II. Structures du type olivine et monticellite. Spectrochimica Acta, 19, 25–47.